TASK QUARTERLY 5 No 3 (2001), 341–353

MICROSCOPIC SIMULATIONS OF NONEQUILIBRIUM CHEMICAL SYSTEMS

JERZY GÓRECKI[1] AND JOANNA NATALIA GÓRECKA[2]

[1] *Institute of Physical Chemistry, Polish Academy of Sciences, Kasprzaka 44/52, 01-224 Warsaw, Poland*
gorecki@ichf.edu.pl

[2] *Institute of Physics, Polish Academy of Sciences, Al. Lotnikow 32/46, 02-668 Warsaw, Poland*
gorec@ifpan.edu.pl

(Received 4 June 2001; revised manuscript received 27 June 2001)

Abstract: In this paper we discuss applications of molecular dynamics in modeling of nonequilibrium effects in chemical systems. We focus our attention on simulations, which use the "reactive" hard spheres technique. We demonstrate that information on nonequilibrium rate constant in a system with a thermally activated reaction can be easily obtained from such simulations. We also present results for a wavefront propagation in a system with an autocatalitic reaction: $A+B \rightarrow A+A$.

Keywords: molecular dynamics, reactive hard spheres, rate constant, chemical wave front

1. Introduction

The standard chemical kinetics is based on equations which describe how the concentrations of reagents evolve in space and time. These equations are written on the basis of the mass action law and the parameters like the rate constants or the diffusion constants come from the experiments. However the rapid development in computational techniques allows one to go beyond this "classical" approach. The methods of quantum mechanics bring information on cross sections corresponding to different reaction channels. The techniques of computational statistical physics allow one to study a system composed of millions of individual particles and consider their interactions at the microscopic level. In the following we focus our attention on this subject.

We think that effective methods of microscopic simulations of chemical systems, based on idealized, model reaction schemes, are important because they play the role of "experiments" in which, contrary to the real case, all the elementary chemical processes are known. At the microscopic level a reaction may be described by an appropriate choice of intermolecular potential, but in the statistical studies it is simpler to associate chemical reactions with close encounters between particles. Such approach is a great simplification, but it reflects the most important aspect of chemistry: only molecules which are close one to another may react. In the most idealized simulations all reagents in the system

are represented by similar geometrical objects and the parameter describing their chemical identity has no influence on the interaction with the other "molecules" (so the chemical identity is like a color). Such simplifications are important because they make the simulation of 10^6 or more particles possible. The most popular simulation techniques are the Bird method [1] and the lattice-gas cellular automata [2]. They are fast enough to give us information on collective phenomena like chemical oscillations [3], front propagation [4] or Turing structures [5], for which characteristic times are much longer than the characteristic time describing intermolecular interactions.

Another useful technique for microscopic simulations of chemical systems is molecular dynamics for reactive hard spheres developed quite a long time ago [6–9]. Molecular dynamics is just a numerical solution of the classical (usually Newtonian) equations of motion for particles interacting via an assumed type of potential [10]. In such approach the diffusion of particles comes out naturally as the result of mutual interaction between them. In molecular dynamics of reactive hard spheres all reagents are described by spheres which can not overlap and can interact only if their distance is equal to the sum of their radii. Such description corresponds to the interaction via a potential which is equal to zero if the distance is higher than a sum of radii and it becomes infinitely large if this distance is smaller. In the most cases it is assumed that the collision between spheres is elastic so the kinetic energy of spheres after the collision is the same as before it. The fact that hard spheres do not interact if they do not collide simplifies simulations a lot: all spheres in the system, except of those which collide, are moving freely in space. Therefore, it is easy to record complete information on system's evolution: it is just enough to save the initial velocities together with times of collisions and post-collision velocities. In practice we can store information on 10^7 consecutive collisions on a single CD.

In typical simulations of "chemically reacting" hard spheres a mechanical motion is fully separated from the chemical properties. So, we can easily introduce different types of "chemical reactions": The most obvious are binary reactions of the type [9]:

$$A + B \rightarrow C + D \tag{1}$$

In such case if two spheres marked as A and B collide they may be instantaneously transformed into the spheres of C and D type. The probability of such transformation may depend on precollision velocities of A and B (for example in order to obtain a thermally activated process [11]) which of course determines the reaction rate. For the hard spheres it is also easy to model an unimolecular reaction of the type:

$$A \rightarrow B \tag{2}$$

by including the probability of a spontaneous transformation of A into B during the motion. It is worth noticing that simulating such transformation in a system of particles interacting via a potential can be more difficult because usually one should consider a change in interactions at the moment it happens.

The model of hard spheres may be also used to describe multimolecular processes, although the procedure is more complex. The time of collision of two hard spheres is precisely equal to zero so the probability of multi-sphere collision is null unless a very special initial condition is selected. If we consider a process:

$$A + A + A \rightarrow B + C + D \tag{3}$$

then it would be meaningless to relate it with a collision of three A spheres. On the other hand, this reaction can be modeled as a binary collision of two A particles with an additional

condition that the third sphere representing A should be closer to the colliding ones than an assumed distance. If so, the particles of A are randomly relabeled as B, C and D. It can be shown that such a procedure describes a trimolecular process [12]. Similarly, one can introduce multiparticle reactions into the simulations based on the hard spheres.

Molecular dynamics for reactive hard spheres allows one for more realistic simulations than the Bird method because it takes the short distance correlations between particles into account. It is also more realistic than the lattice-gas automata because it does not introduce any restrictions on the direction and on the value of particle's velocity. On the other hand, molecular dynamics simulations are more time consuming than the other techniques mentioned above. A step towards more efficient simulations was suggested in [13] and then it was successfully used to calculate the influence of nonequilibrium effects on the rate constant in a system with a thermally activated reaction [14]. It was based on an observation that if one considers only thermoneutral reactions then a trajectory of a chemical system is the same as for an equilibrated system of hard spheres. Thus, many different chemical systems may be studied using the same equilibrium trajectory by assuming different reaction schemes and assigning the chemical identity parameters to particles in a different way.

The method mentioned above gives reaction paths for a chemical system with the same number of particles as the one for which the equilibrium trajectory was recorded. However, if the equilibrium trajectory is obtained for the periodic boundary conditions, then a spatial extension of system's size is possible. The periodic boundary conditions mean that the simulated system is regarded as an elementary cell in an infinite system, which is invariant with respect to translations by vectors corresponding to cell's edges. Knowing the evolution within a single (elementary) cell we have the information about positions and velocities for particles in the whole system. Therefore, a prerecorded trajectory gives us the evolution of a system which is expanded by a number of edge lengths in each direction. Of course, the periodic boundary conditions remain satisfied for the expanded system. If chemical identities of molecules are neglected than such expansion does not bring us any new information, as the motion in all replicas of the elementary cell is identical. Moreover, it may lead to wrong conclusions because the correlations extending over a single cell are affected by artificially introduced periodicity. However, for a multicomponent chemical system, in which the motion is not related to chemical identity, the situation is different. First, various chemical compositions may be initialized in miscellaneous cells by marking the equivalent (by periodicity) spheres in a different way. Secondly, a steric factor (reaction cross section), if it is not equal to unity, differentiates the time evolution in various cells, because a collision between the equivalent particles may be reactive in one cell and nonreactive in another. Because of the periodic boundary conditions a free flow of molecules between the neighboring cells is ensured. Thus, one obtains the evolution of a system which is much larger than the original one. Let us also notice that the number of collisions per particle, which decides about the time scale of simulated processes, is the same for both the original and the expanded systems. This method [15] is extremely efficient from the computational point of view. When an expanded system is created one needs only one large array to store the chemical identities of all particles (one may use logical or short integer variables), whereas the other quantities as velocities, positions and moments of collisions are periodic in space and they do not require a large memory. In practice a personal computer may easily manage simulations involving 10^7 particles.

In the following two sections we would like to present two applications of the molecular dynamics for reactive hard spheres. The first is concerned with the nonequilibrium rate constant in a system with a thermally activated reaction. The second shows the simplest organized spatio-temporal chemical structure – a wavefront crated by an autocatalitic process: $A+B \rightarrow A+A$.

2. Molecular dynamics simulations of nonequilibrium effects associated with a thermally activated reaction

It was recognized a long time ago [16] that thermally activated chemical reactions may create nonequilibrium energy distributions of their reactants because the reaction cross section strongly depends on the energy of interacting molecules. The deviation of the energy distribution function from its equilibrium form changes the value of the rate constant. The influence of the nonequilibrium effects related to a thermally activated reaction on system's evolution has been intensively studied. Most of the theoretical approaches are concerned with single thermoneutral reaction of the form [17–21]:

$$A+A \rightarrow B+C \tag{4}$$

which proceeds in a system of hard spheres. If the process starts with an equilibrium distribution of A particles then the nonequilibrium effects decrease the rate constant of the reaction with respect to its equilibrium value because the most energetic molecules of the reactant are transformed into products in a more efficient way than the less energetic ones. The theoretical studies [16–21] are based on the Boltzmann equation, which is generalized to take the reaction into account. Some analytical results for the nonequilibrium rate constants have been obtained for so called line-of-center model of the reaction cross section (σ^*) [11]. According to it:

$$\sigma^* = \begin{cases} \frac{1}{4} s_F d^2 \left(1 - \frac{E_A}{E_C}\right) & \text{for } E_C \geq E_A \\ 0 & \text{for } E_C < E_A \end{cases} \tag{5}$$

where E_A is the activation energy, d and m denote the diameter and mass of a sphere and $E_C = \frac{1}{4}(\vec{v}_1 - \vec{v}_2)^2 m$ where $\vec{v}_1$ and $\vec{v}_2$ are the velocities of colliding spheres. s_F is the steric factor and it scales the probability of reaction. It can be shown that if the velocity distribution of A spheres is Maxwellian and if it corresponds to the temperature T ($f_T^{(M)}$) then the rate constant equals to:

$$\int f_T^{(M)}(\vec{v}_1)\sigma^* f_T^{(M)}(\vec{v}_2) d\vec{v}_1 d\vec{v}_2 = s_F 4 d^2 \left[\frac{\pi k_B T}{m}\right]^{\frac{1}{2}} \exp\left[-\frac{E_A}{k_B T}\right], \tag{6}$$

which is just the Arrhenius law [22].

Although, the Arrhenius law is common for thermally activated reactions the cross section as the function of energy usually has more complex form than that given by Equation (5). For example for a thermally activated ion-molecule reactions a typical reaction cross section has a shape shown in Figure 1 ([23]). For our simulations we approximated this shape by the following function:

$$\sigma^* = \begin{cases} 5\left(\frac{E_C}{E_B} - 1\right)\exp\left(-\frac{E_C}{E_B}\right) & \text{for } E_C \geq E_B \\ 0 & \text{for } E_C < E_B \end{cases} \tag{7}$$

and we selected $E_B = 5k_B T_0$. The rate constant which corresponds to the cross section (7), as the function of the inverse temperature (in T/T_0 units), is shown in Figure 2. It was

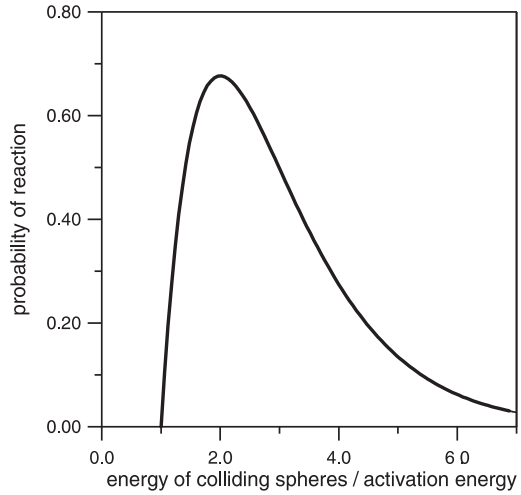

Figure 1. The considered reaction cross section σ^* as a function of $\frac{E_C}{E_B}$

obtained by summing up σ^* (Equation (7)) for all collisions in simulations performed at different temperatures. In the simulations we used 2744 spheres with the packing density $\eta = 0.155$. It is interesting that in a wide range of temperatures (from $0.4T_0$ to $1.2T_0$) the dependence of the rate constant on temperature is correctly described by Equation (6). The best numerical fit corresponds to $E_A = 4.1 k_B T_0$.

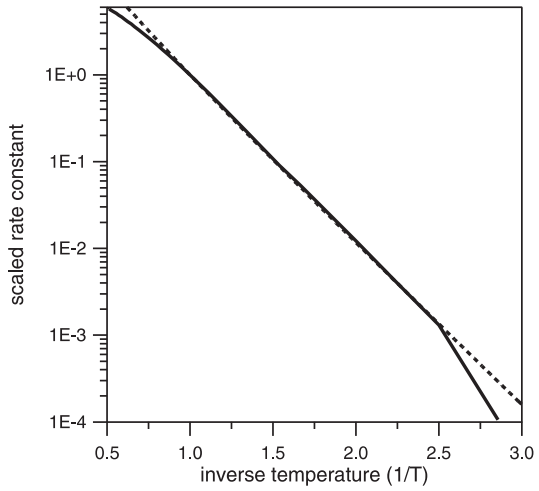

Figure 2. The solid line shows the rate constant obtained for the cross section (7) (scaled to its value for the temperature T_0) as a function of the inverse temperature (T_0/T). Let us notice that in a wide range of temperatures (from $0.4T_0$ to $1.2T_0$) the dependence of rate constant can be correctly described by Equation (6). The best fit (the dashed line) corresponds to $E_A = 4.1 k_B T_0$

Now let us consider the nonequilibrium rate constant in a system which at the beginning is composed of the equilibrated molecules of A only. Let the initial temperature of the system be T_0. The time dependent rate constant may be calculated from the average time the system spends in the state characterized by N_A molecules of reactant A [14].

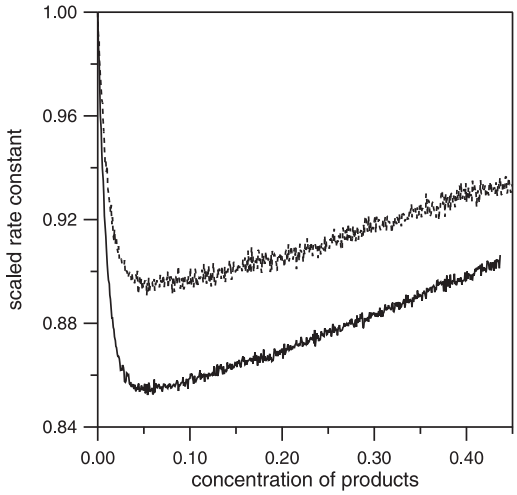

Figure 3. The solid line shows the nonequilibrium rate constants for reaction (4) with the reaction cross section (7) as the function of the concentration of products. The value of the rate constant is scaled to its equilibrium value at the temperature T_0. The dashed line shows the nonequilibrium rate constant for the line-of-center model which approximates the equilibrium rate constant of the original process

Reaction (4) is unidirectional, so it is convenient to use the total concentration of products as the measure of reaction progress. The results are presented in Figure 3. The solid line shows the rate constants for reaction (4) with the reaction cross section (7). The value of the rate constant is scaled to its equilibrium value at the temperature T_0. As expected, the rate constant is rapidly decreasing at the initial stage of reaction because the most energetic molecules of A are transformed into products. Next it starts to increase again because the energy is transferred back to the reactant due to collisions between reactant and products. Usually the experimental results bring us information on the activation energy of a given process. Is this information sufficient to estimate the nonequilibrium rate constant? The dashed line shows that the answer is negative. It was obtained for the line of center model (the reaction cross section (5)) which gives a good approximation for the temperature dependent equilibrium rate constant of the original process ($E_A = 4.1 k_B T_0$, see Figure 2). The steric factor for this line of center model (s_F in Equation (5)) was selected such a way that the equilibrium rate constants of both reactions at the temperature T_0 are equal. The simulations show that the nonequilibrium rate constants for both processes are different. It demonstrates that in order to obtain the nonequilibrium rate constant one has to have detailed information on the reaction cross section.

3. Molecular dynamics simulations of a chemical wavefront propagation

A propagating chemical wave front, which consumes reactants ahead and leaves products behind is one of the simplest manifestations of an organized spatio-temporal structure in a nonhomogeneous chemical system. One of the most widely studied examples of a chemical wave front is related to quadratic autocatalysis [24–27]:

$$A + B \xrightarrow{k} A + A \tag{8}$$

Reaction (8) was originally introduced to describe the spread of a favored genetic trait A through a population of B. In chemistry a quadratic autocatalytic process is included in many simple models of nonlinear systems such like the models of Lotka [28], Lotka-Volterra [29] or the reduced model of the Ce(III) bromide reaction [30]. The terms related to quadratic autocatalysis appear also in the kinetic equations describing real chemical processes like for example chlorite-iodide reaction [31]. For reaction (8) both states: composed of pure A molecules and composed of pure B molecules are stationary; the first one is stable and the other is unstable. Therefore, in a nonhomogeneous system the interface between A and B propagates into the region composed of pure B. It follows from the reaction scheme (8) that the total number of molecules of A and B remains constant. Let us denote a and b the concentrations of corresponding species and let n_0 be the total concentration of them ($a+b=n_0$). Having in mind that at each space point x and at every time moment t one has $a(x,t)+b(x,t)=n_0$, the state of the system is defined if a single concentration only, for example, $a(x,t)$, is known. The time evolution of a system with reaction (8) is described by the reaction-diffusion equation, which has the form [26]:

$$\frac{\partial a}{\partial t} = kab + D\nabla^2 a = ka\,(n_0 - a) + D\nabla^2 a, \tag{9}$$

where k and D denote the rate constant and the diffusion constant, respectively. Introducing the scaled variables: concentration $\alpha = a/n_0$, rate constant $\kappa = n_0 k$, time $\tau = \kappa t$ and the space variable $\xi = \sqrt{\kappa/D}r$ one can transform Equation (9) to the form:

$$\frac{\partial \alpha}{\partial \tau} = \alpha\,(1-\alpha) + \nabla^2\alpha. \tag{10}$$

For the moment let us focus our attention on one-dimensional systems only. Let us consider a stationary wave front propagating along the x-axis with a constant velocity v. Its profile may be described in the reference frame moving together with it:

$$\alpha(\xi,\tau) = \alpha(\xi_x,\tau) = \alpha(\xi), \tag{11}$$

where $\xi = \xi_x - v\tau$. The front profile α as a function of ξ variable satisfies equation:

$$v\frac{\partial \alpha}{\partial \xi} + \frac{\partial^2 \alpha}{\partial \xi^2} + \alpha(1-\alpha) = 0. \tag{12}$$

Because of the mathematical simplicity of Equation (9) the wave front propagation in system with reaction (8) has been intensively studied. It is known [26] that Equation (12) admits solutions, which are stable with respect to local perturbations for all velocities which are greater than or equal to the critical one $v_{\min} = 2$ which condition in non-scaled variables transforms to:

$$v_{\min} = 2\sqrt{\kappa D}. \tag{13}$$

The particular solution of Equation (12) which corresponds to $v_{\min}$ is very important because it was shown by Mc Kean [32] that a step-function initial distribution of A evolves into a wave front propagating with this minimal velocity. This results was later generalized by Bramson [33] and Merkin and Needham [34] who proved that velocity of any front originating from an initial condition, such that the concentration of A vanishes for all ξ greater than ξ_0 converges to the minimal stable velocity. Unfortunately the analytical solution for the profile corresponding to $v_{\min}$ is not known.

If one relates reaction (8) to binary collisions in a system of A and B particles then its rate may be described as:

$$k = s_F k_0, \tag{14}$$

where k_0 is the rate of binary collisions and s_F is the steric factor, which says what is the probability that an encounter of A and B particles ends with a reaction. Finally the minimal stable velocity can be expressed as:

$$v_{\min} = 2\sqrt{s_F n_0 k_0 D}. \tag{15}$$

In our simulations of a propagating wave front we use the periodic expansion of pre-recorded equilibrium trajectory [15]. We considered a couple of different systems with packing fractions ranging from $\eta = 0.128$ to $\eta = 0.238$. A typical number of particles in the equilibrium trajectory exceeds 1000. Such an equilibrium system was periodically expanded by a few side lengths in x and y directions and by more than 80 side lengths in the z direction. Usually the total number of spheres used in our simulations N exceeds 2 000 000. For an expanded system the periodic boundary conditions were used in x- and y-directions. In order to observe front propagation the initial concentration of reagents were inhomogeneous in the z-direction. Part of the simulations started from the initial concentrations described by a step-function: all spheres for which $z \leq z_0$ were marked as A, all the others as B. In these simulations z_0 corresponded to 15 side lengths. In other simulations there was a wide interval of z within which the initial concentrations of both reagents were different from zero. We have found that the initial condition has no influence on the observed stable velocity of a front. A modified periodic boundary conditions were used in the z-direction of the expanded system. They mean that a particle of A, which left the expanded system at $z = 0$ entered the system from the other end as a particle of B and *vice versa*. To analyze the results, the system was divided into slices perpendicular to the z-axis (200 slices were used). The fraction of particles of each reactant was averaged over each slice. In order to study the influence of reagent's concentration (n_0) on the front velocity one can also introduce neutral (solvent) particles into the system and they do not take part in the reactions. Of course, the boundary conditions for such particles are periodic. In our analysis of a front propagation we use the average concentrations of A in a slice perpendicular to the z axis. Typical snapshots of a propagating wave front are shown in Figure 4. These results were obtained for a system in which 60% of spheres represented a solvent. At the beginning reactant A and a solvent were initialized at the left hand side of the system, whereas only B and solvent particles were on the right. A stable profile of concentration of A (the long and short dashed lines) propagates to the right. One can measure the progress of the front by observing the position of a specific point on the front's profile as the function of time. This method is the most popular and has been used by many authors [35]. However it not very accurate and here we use more precise approaches.

The values of α and $\beta = 1 - \alpha$ can be precisely defined for each slice at any time t. We introduce a new quantity $\gamma(z)$ as:

$$\gamma(z_i,t) = \begin{cases} \alpha(i,t), & \text{if } \alpha(i,t) \leq 0.5 \\ \beta(i,t), & \text{if } \alpha(i,t) > 0.5 \end{cases}, \tag{16}$$

where z_i is the mean value of z corresponding to the i-th slice. $\gamma(z,t)$ is localized function of z. We can define the front position as:

$$< z > (t) = \frac{\sum_i z_i \gamma(z_i,t)}{\sum_i \gamma(z_i,t)}. \tag{17}$$

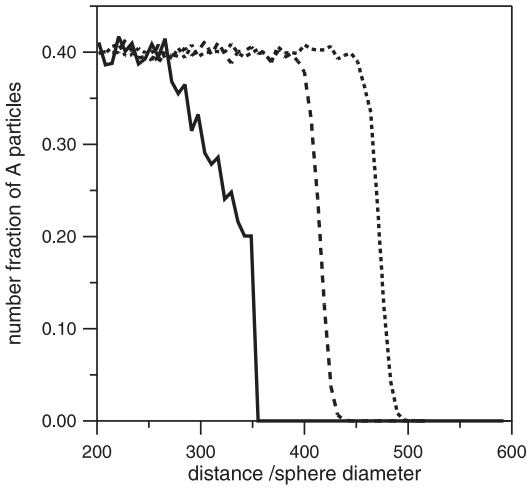

Figure 4. Three snapshots of a propagating front. Results for $s_F = 0.1$, $\eta = 0.128$ and $N = 2\,000\,000$. The curves from left to right (decreasing dash length) correspond to increasing time

Alternatively, one can study the number of A particles as a function of time. The system's density does not change in time so the increase in number of A can be transformed into the volume covered by the front and thus for the distance traveled. The results of both methods for a front generated by a reaction with $s_F = 0.05$ in a system with packing fraction $\eta = 0.238$ are shown in Figure 5. The upper curve (marked with crosses) shows $< z > (t)$, whereas the lower curve (marked with circles) represents the position of a front calculated from the volume of created A particles. The lower curve is shifted down by 30 sphere diameters to make it distinguishable from the upper one. The front velocities calculated from the upper and lower curves are in perfect agreement as they are equal to 0.3432 and 0.3414 $\frac{d}{ps}$, respectively.

It is known that the velocity of an autocatalytic front is decided by the region in which the concentration of A is very small. In simulations we have a natural cutoff for the nonzero number fraction of A – the number of A particles in a slice can not be smaller than 1 so, roughly speaking, the minimum number fraction of A is 1/[number of spheres in a slice]. A number of tests for different system sizes have been performed and the results are shown in Figure 6. We have not observed any regular influence of system size on front's velocity. Moreover, the results obtained from simulations in which the systems was expanded by 3 or more boxes in x- and y-directions are practically the same.

The velocity of a front as a function of the number fractions of the reagents A and B is shown in Figure 7. The steric factor for the considered reaction was 0.1 and the simulations were performed for a system of $N_0 = 1000$ particles with packing fraction $\eta = 0.128$ which was periodically expanded by 5, 5 and 80 boxes in the x, y and z directions, respectively. From Equation (15) we obtain the following expression for v_{min} in a system with solvent:

$$v_{min} = 2\sqrt{s_F n_0 k_0 D} = 2\sqrt{s_F (n_A + n_B + n_S) k_0 D}\sqrt{\frac{n_A + n_B}{n_A + n_B + n_S}}. \tag{18}$$

For simulations based on a single pre-recorded trajectory the first term is constant and thus the velocity is a linear function of the square root from the total number fraction of the reagents A and B. Such linear dependence can be seen on Figure 7 in the whole range of

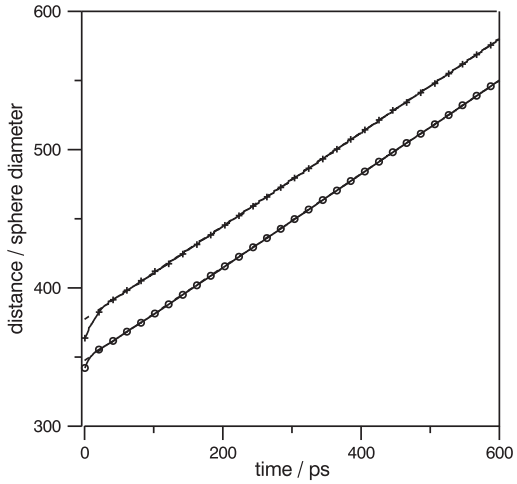

Figure 5. Front's position as a function of time; results for $s_F = 0.05$, $\eta = 0.238$ and $N = 5\,488\,000$. The upper curve (crosses) – $< z > (t)$, the lower curve (circles) – the position of a front calculated on the basis of the volume of created A particles (shifted down by $30d$). The dashed curves show linear fits of front position; the velocities calculated from the upper and lower curves are equal to 0.3432 and 0.3414 $\frac{d}{ps}$, respectively

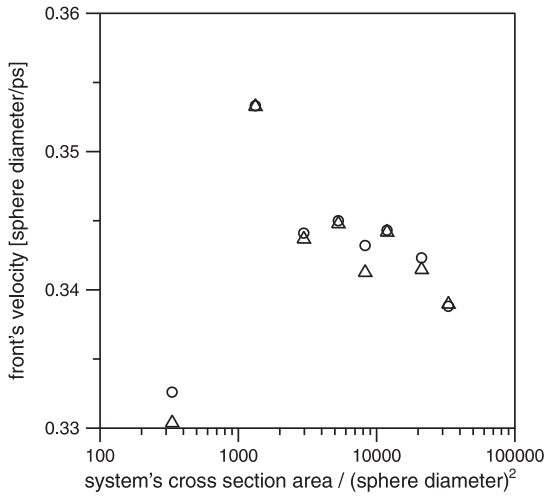

Figure 6. Front's velocity as a function of system's size; results for $s_F = 0.05$, $\eta = 0.238$. The considered systems were expanded by 80 box lengths in the direction of wave propagation. In the perpendicular directions we considered an unexpanded system as well as the systems expanded by 2, 3, 4, 5, 6, 8 and 10 box lengths (there were 21 952 000 spheres in the last one!). The circles and triangles show the velocity calculated from $< z > (t)$ and from the increase in the volume occupied by A particles, respectively

studied concentrations of active reagents. Using the molecular dynamics data we can easily calculate k_0, D and $n_A + n_B + n_S$ ($k_0 = 5.5\frac{d}{ps}$, $D = 0.369\frac{d^2}{ps}$, $n_A + n_B + n_S = 0.244d^{-3}$). Therefore the factor $2\sqrt{s_F(n_A + n_B + n_S)k_0 D} = 0.448\frac{d}{ps}$ and the coefficient describing the linear fit of the molecular dynamics data equals $0.422\frac{d}{ps}$. The agreement between both numbers is very good. Therefore, our computer experiments indicate that even very fast reactions in the system of low density (we considered $s_F = 0.1$ which means that 10% of all collisions

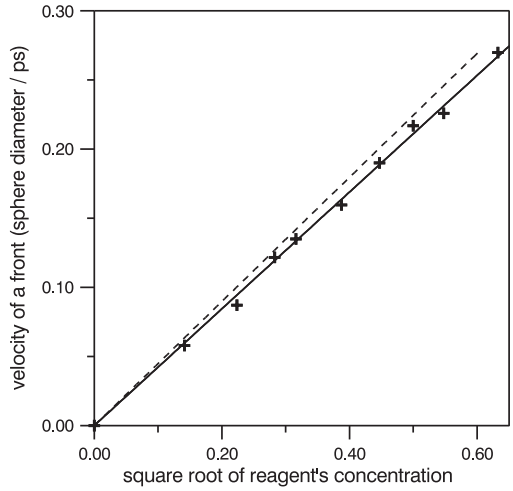

Figure 7. The velocity of a front as a function of the square root from total number fraction of the active reagents in the system. Crosses denote molecular dynamics results, the solid line shows their best linear fit and the dashed line is drown using Equation (15). Results for $s_F = 0.1$, $\eta = 0.128$ and $N = 2\,000\,000$. All values nicely follow a straight line, however its coefficient is by a few percent smaller than predicted by the theory

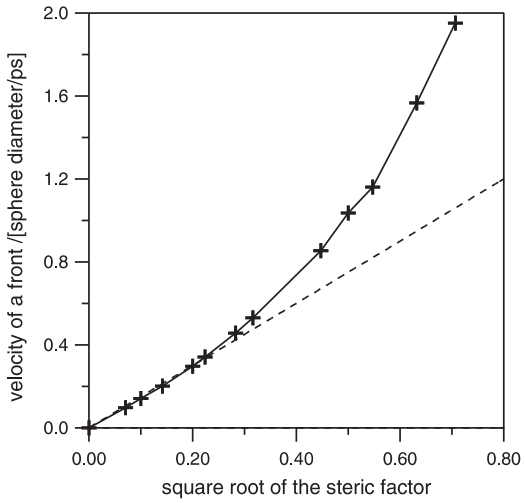

Figure 8. The velocity of a front as a function of the square root from the steric factor. Crosses denote molecular dynamics results and the dashed line is drown using Equation (15). Results for $\eta = 0.238$ and $N = 5\,488\,000$

between A and B leads to a reaction) can be accurately described by the reaction-diffusion Equation (9).

Now let us consider a system with higher density and let us discuss the front velocity as a function of the steric factor. Here we assume that the system is composed of A and B molecules only. One can feel that for a reaction proceeding in a dense system the formula for the minimum stable velocity fails. There are a few reasons for it. First, if reaction is fast than diffusion of particles is not given by Fick's law and one should take the relaxation of

concentration gradients to diffusion into account. We have estimated this effect on the basis of extended irreversible thermodynamics, showing that the hyperbolic diffusion terms should increase front velocity [36]. Next, one can easily see that the Equation (15) fails when the system density is high. Let us consider an ansamble of disks arranged in a regular quadratic lattice on a plane and let the distances between the particles are only slightly larger than their diameter. Of course, in such a case each particle is trapped inside the cage generated by its neighbors and thus the diffusion constant is zero, so according to Equation (15) a front does not move. On the other hand if we mark all the disks left of a given point as A and all right of it as B and allow for reaction (8) then the front will propagate to the right as after each reaction it moves by a sphere diameter. One can estimate that the motion of a front in a dense system should be proportional to the rate constant (but not to its square root as in Equation (15)). We have performed a set of computer experiments for a system with $\eta = 0.238$. A few systems with different number of molecules have been considered, just to check if the results are consistent. The velocity of a front as a function of the square root from reaction's steric factor is presented in Figure 8. It can be seen that the range of steric factors for which the velocity is given by Equation (15) is very narrow and ends at $s_F = 0.1$ ($\sqrt{s_F} \sim 0.3$). Next the front velocity as a function of the steric factor grows much faster and the effects behind it (the finite size of a molecule, the hyperbolic diffusion) are not included it the standard reaction-difusion equation.

4. Conclusions

In this paper we have shown that microscopic simulations may help in better understanding of the properties of systems with chemical reactions. But, as the matter of fact, we can get much more from them. It is known that spatial correlations between different reagents may appear in a nonequilibrium chemical system [37] and the molecular dynamics for reactive hard spheres is a perfect tool to measure them. Microscopic simulations contain information on the evolution of every molecule in the system so we can study fluctuations and their influence on systems dynamics. Therefore, we can test not only the theories which describe the time evolution of the average quantities, but also such approaches which include stochastic methods like master equation or stochastic differential equations ([38]). An example of such work is the study on fluctuation induced transitions in a spatially distributed system with a model enzymatic reaction ([39]).

References

[1] Bird G A 1976 *Molecular Gas Dynamics* Clarendon Oxford
[2] Kapral R 1991 *J. Math. Chem.* **6** 113;
Kapral R, Lawniczak A and Masiar P 1991 *Phys. Rev. Lett.* **66** 2539
[3] Mareschal M and De Witt A 1992 *J. Chem. Phys.* **96** 2000;
Malek-Mansour M and Baras F 1992 *Physica* **A 188** 253;
Wu Xiao-Guang and Kapral R 1994 *J.Chem.Phys.* **100** 5936
[4] Lemarchand A, Nowakowski B and Karzazi M A 1998 *Acta Phys. Pol.* **29** 1623;
Lemarchand A and Nowakowski B 1998 *Europhys. Lett.* **41** 455;
Lemarchand A and Nowakowski B 1999 *J. Chem. Phys.* **111** 6190;
Lemarchand A and Nowakowski B 2000 *J. Phys. Rev.* **E 62** 3156
[5] Kapral R, Lawniczak A and Masiar P 1992 *J. Chem. Phys.* **96** 2762
[6] Turner J S 1977 *J. Phys. Chem.* **81** 2379
[7] Gillespie D T 1977 *J. Phys. Chem.* **81** 3240
[8] Boissonade J 1982 *Physica* **A 113** 607

[9] Górecki J and Gryko J 1989 *Computer Phys. Comm.* **54** 245
[10] Allen M P and Tidesley D J *Computer Simulations of Liquids* Clarendon Press, Oxford
[11] Present B D 1959 *J. Chem. Phys.* **31** 747
[12] Górecki J 1994 *Molecular Dynamics Simulations of Nonequilibrium Effects in Chemical Systems* in "Far-from-Equilibrium Dynamics of Chemical Systems", Eds.: Górecki J, Cukrowski A S, Kawczyński A L and Nowakowski B World Scientific Singapore
[13] Der R and Fritzche S 1985 *Chem. Phys. Lett.* **121** 177
[14] Górecki J, Popielawski J and Cukrowski A S 1991 *Phys. Rev.* **44** 3791
[15] Górecki J 1995 *Molecular Physics Reports* **10** 48
[16] Prigogine I and Xhrouet E 1949 *Physica* **15** 913
[17] Ross J and Mazur P 1961 *J. Chem. Phys.* **35** 19
[18] Shizgal B and Karplus M 1970 *J. Chem. Phys.* **52** 4262; *ibid* 1971 **54** 4257; *ibid* 1971 **54** 4345
[19] many papers on this subject can be found in the volumes of *Proceedings of the International Symposium on Far-from-Equilibrium Dynamics of Chemical Systems* Eds. Popielawski J, Górecki J 1991 World Scientific, Singapore and Eds. Górecki J, Cukrowski A S, Kawczyński A L and Nowakowski B 1994 World Scientific, Singapore
[20] Napier D G and Shizgal B D 1995 *Phys. Rev.* **E 52** 3797
[21] Shizgal B D and Napier D G 1996 *Physica* **A 233** 50; the authors give a comprehensive bibliography on theory of nonequilibrium effects related to the simplest binary reactions
[22] Stiller W 1989 *Arrhenius Equation and Non-Equilibrium Kinetics* Teubner-Texte zur Physik, Band 21, Leipzig
[23] Hirata K and Kebarle P 1975 *J. Chem. Phys.* **63** 394
[24] see for example Kapral R and Showalter K 1995 *Chemical Waves and Patterns* Kluwer
[25] Fisher R A 1937 *Ann. Eugenics* **7** 335;
Kolmogorov A, Petrovsky I and Piskunov N 1937 *Bull. Univ. Moscow Ser. Int. Sec.* **A1** 1
[26] Gray P, Showalter K and Scott S K 1987 *Journal de chimie physique* **4** 1329
[27] Ebert U and van Saarloos W 2000 *Physica* **D 146** 1
[28] Lotka A J 1910 *J. Phys. Chem.* **14** 271
[29] Lotka A J and Volterra V 1931 *Lecons sur la Theorie Mathemathiques de la Lutte pour la Vie* Paris
[30] Noyes R M 1980 *J. Chem. Phys.* **72** 3454
[31] De Kepper P, Boissonade J and Epstein I R 1990 *J. Phys. Chem.* **94** 6525
[32] Mc Kean H P 1975 *Comm. Pure Appl. Math.* **28** 323
[33] Bramson M D 1978 *Comm. Pure Appl. Math.* **31** 531
[34] Merkin J H and Needham D J 1989 *J. Engineering Mat.* **23** 343
[35] Velikanov M V and Kapral R 1999 *J. Chem. Phys.* **110** 109
[36] Górecki J 1995 *Physica* **D 84** 171;
Górecki J and Górecka J N 1998 *Acta Physica Polonica* **B 29** 1663
[37] Kuramoto Y 1974 *Prog. Theor. Phys.* **52** 711;
Nicolis G and Malek M 1984 *Mansour, Phys. Rev.* **A 29** 2845;
Kitahara K, Seki K and Suzuki S 1990 *J. Phys. Soc. Japan* **59** 2309;
Nicolis G, Amellal A, Dupont G and Mareschal M 1989 *Journal of Molecular Liquids* **41** 5;
Górecki J, Kitahara K, Yoshikawa K and Hanazaki I 1994 *Physica* **A 211** 327
[38] van Kampen N G 1987 *Stochastic processes in physics and chemistry* North-Holland, Amsterdam;
Gardiner C W 1987 *Handbook of stochastic methods* Springer, Berlin
[39] Górecki J, Kawczyński A L and Nowakowski B 1999 *J. Phys. Chem.* **A 103** 3200